separations

MDPI

Communication

Postmortem Internal Gas Reservoir Monitoring Using GC×GC-HRTOF-MS

Pierre-Hugues Stefanuto [1,*], Katelynn A. Perrault [1], Silke Grabherr [2], Vincent Varlet [3] and Jean-François Focant [1]

1 Organic and Biological Analytical Chemistry Group, Chemistry Department, University of Liège, Allée du 6 Août 11 (Bât B6c), Quartier Agora, 4000 Liège (Sart-Tilman), Belgium; katelynn.perrault@ulg.ac.be (K.A.P.); jf.focant@ulg.ac.be (J.-F.F.)

2 Forensic Anthropology and Imaging Unit, University Center of Legal Medicine, Chemin de la Vulliette 4, CH-1000 Lausanne 25, Switzerland; silke.grabherr@chuv.ch

3 Forensic Toxicology and Chemistry Unit, University Center of Legal Medicine, Chemin de la Vulliette 4, CH-1000 Lausanne 25, Switzerland; vincent.varlet@chuv.ch

* Correspondence: phstefanuto@ulg.ac.be; Tel.: +32-4-366-34-30

Academic Editor: Shari Forbes

Received: 8 April 2016; Accepted: 3 August 2016; Published: 17 August 2016

Abstract: Forensic investigations often require postmortem examination of a body. However, the collection of evidence during autopsy is often destructive, meaning that the body can no longer be examined in its original state. In order to obtain an internal image of the body, whole body postmortem computed tomography (PMCT) has proven to be a valuable non-destructive tool and is currently used in medicolegal centers. PMCT can also be used to visually locate gas reservoirs inside a cadaver, which upon analysis can provide useful information regarding very volatile compounds that are produced after death. However, the non-targeted profiling of all potential volatile organic compounds (VOCs) present in these reservoirs has never been attempted. The aim of this study was to investigate the VOC profile of these reservoirs and to evaluate potential uses of such information to document circumstances surrounding death, cause of death and body taphonomy. Comprehensive two-dimensional gas chromatography coupled to time-of-flight high-resolution mass spectrometry (GC×GC-HRTOF-MS) was used for VOC measurements. This study demonstrated that the chemical composition of VOCs within the gas reservoirs differed between locations within a single body but also between individuals. In the future, this work could be expanded to investigate a novel, non-destructive cadaver screening approach prior to full autopsy procedures.

Keywords: human decomposition; forensic chemistry; comprehensive two-dimensional gas chromatography coupled to time-of-flight high-resolution mass spectrometry (GC×GC-HRTOF-MS); volatile organic compounds; multivariate statistics

1. Introduction

Postmortem imaging techniques are commonly used prior to an autopsy for forensic investigations. These techniques allow some information to be collected and saved prior to their possible destruction and loss due to the invasiveness of the autopsy procedure. Whole body postmortem computed tomography (PMCT) is often used as the imaging technique in postmortem examination. It allows the visualization of internal characteristics of the body and can serve to detect the precise localization of gas reservoirs present inside the body and further allow their collection [1–5]. Routinely, the occurrence and the distribution of postmortem gases are used in medicolegal laboratories, often to provide information about the cause of death [5,6]. However, the full chemical composition of these reservoirs has never been analyzed [5]. This lack of chemical profiling could lead to the misinterpretation of

the origin of these gases. For example, the chemical profile of this gas could potentially discriminate between putrefactive gas buildup and the occurrence of a gas embolism [6]. In 2015, Varlet et al. demonstrated the possibility to chemically differentiate alteration gases and gas embolisms using gaseous compositions (e.g., O_2, N_2, CO_2, CH_4, and H_2S) [5]. In order to obtain more information regarding the cause of death or the postmortem interval (PMI), a complete screening of the volatile organic compounds (VOCs) present in these gas reservoirs would be extremely valuable.

Comprehensive two-dimensional gas chromatography (GC×GC) techniques have already been reported to be of high efficacy for the monitoring of decomposition VOCs from different matrices such as soils [7–11] and whole body headspace [12–19]. An increase in separation power is required to efficiently separate the hundreds of VOCs emitted by decomposing remains. Moreover, the hyphenation of GC×GC with mass spectrometry also provides identification information based on signal deconvolution and compound-specific fragmentation patterns. When high-resolution time of flight mass spectrometry (HRTOF-MS) is used, the high mass measurement accuracy additionally contributes to better tentative identifications of compounds present in the mix of decomposition volatiles [11].

Considering PMCT gas reservoir sampling in combination with the separation power of GC×GC and the mass measurement accuracy of HRTOF-MS is a pioneering approach for comprehensive screening of the chemical composition of internal gas reservoirs within a dead body. For the present study, internal gases were sampled under laser guidance and assisted by postmortem multi-detector computed tomography (MDCT) following an established procedure [4,5,20]. Solid-phase microextraction (SPME) was applied to concentrate and to introduce the VOCs into the chromatographic system. GC×GC-HRTOF-MS was then used in order to obtain good separation and robust identification of the compounds of interest. The primary objective was to demonstrate the ability of SPME GC×GC-HRTOF-MS to detect low-level VOCs from internal gases. The combination of various statistical approaches was then investigated to provide information regarding the decomposition status of organs within a body.

2. Materials and Methods

2.1. Sampling

2.1.1. Internal Gas Sampling

First, the location of each intracadaveric gaseous reservoir was revealed during PMCT. In each reservoir, a needle equipped with a closed three-way tap was introduced through the body and into the reservoir, which was facilitated by radiological guidance using three-dimensional coordinates in biopsy mode. A second control computed tomography scan (CT-Scan) was then performed to check the position of the needles in each reservoir. Finally, the three-way tap inserted in each reservoir was slowly opened to withdraw gas into a Luer-lock polytetrafluoroethylene (PTFE) syringe. The three-way taps were then closed and the syringe, tap and needle from each reservoir were removed from the body. The gas samples were then individually transferred from the syringe into a 20 mL headspace vial containing water [4,21,22], where water was expelled to compensate for the introduction of gas volume. A residual water quantity was left in each vial to permit complete seal. Vials were inverted and stored at +4 °C prior to analysis. Preliminary studies were conducted on gases and have assured sample stability over a minimum period of two months while refrigerated [5].

The sampling and storage of gas is complex and even more so in the specific case of forensic evidence. This procedure for collecting gas reservoirs has already been implemented during the medico-legal investigation of the bodies [4,21,22]. Thus, the samples for this study were collected in the same manner in order to allow several analyses to be performed on the same sample. The partitioning of the most polar compounds into the water phase was expected; however, this effect was not characterized within this study. The partitioning between the aqueous and the gas phase can be an issue if the biomarkers have high solubility in water, reducing their presence in the gas phase

compared to less polar compounds. A further evaluation of this effect would be necessary after the validation of marker compounds.

2.1.2. VOC Sampling

Once internal gases were trapped in headspace vials, VOCs were sampled using solid phase micro-extraction (SPME) which was an ideal sampling approach given the limited gas volume of each sample. The fiber was coated with 100 µm of polydimethylpolysiloxane (PDMS) (23 ga., Supelco, Belfonte, PA, USA). The PDMS fiber was chosen for this initial screening for its hydrophobic properties, due to high water content within the vials. The fiber was exposed to the gas sample for 15 min at room temperature (i.e., 20 °C). The main practical limitation for SPME was the minimal space (2 cm) available to expose the fiber in the gaseous volume above the water, which was limited by the volume of gas in each reservoir available to be sampled into the vial. Following this proof of concept, a deeper investigation into the equilibrium exchange between the gas and the water phase would provide additional information about VOC concentrations (e.g., using different SPME fibers, SPME in immersion, multiple SPME extraction, or by other chromatographic methods). All gas samplings were performed with ethical agreement (Ethics Committee of Canton de Vaud, Protocol 181/12). Information regarding each cadaver can be found in Table 1.

Table 1. Information regarding the human bodies analyzed in this study.

Body #	Gender	Age	Internal Gas Cavities Location	Cause of Death	Last Time Seen Alive
Body 1	M	32	Pectoral muscle, Left lung, Right lung Pericardium, Abdominal cavity	Suicide by neuroleptics and solvent abuse	2 weeks
Body 2	M	67	Abdominal cavity, Heart	Undetermined	Minimum 1 week
Body 3	F	75	Heart, Abdominal cavity, thorax cavity (2 times)	Undetermined (known cardiac pathologies)	N/A (minimum several weeks)
Body 4	M	68	Subcutaneous, Abdominal cavity, Pericardium, Jugular, Pectoral muscle	Undetermined (known cardiac pathologies)	10 days

2.2. Sample Analysis and Data Processing

The analytical method was based on previously used techniques for whole body decomposition VOC analysis and are described briefly herein [11]. The instrument used was an Agilent 7890A gas chromatograph (Agilent Technologies, Palo Alto, CA, USA) coupled with an AccuTOF™ GCv 4G HRTOF-MS (JEOL Ltd., Tokyo, Japan). A Rxi-5Sil MS first dimension (^{1}D) column (30 m × 0.250 mm ID × 0.25 µm df, Restek Corporation, Bellefonte, PA, USA) and a Rxi-17Sil MS second dimension (^{2}D) column (2 m × 0.250 mm ID × 0.25 µm df, Restek Corporation) were used. Modulation between columns was performed using a ZX2 dual-stage thermal loop modulator (Zoex Corporation, Houston, TX, USA). The cold jets were cooled by the ZX2 system to −90 °C and hot jets were maintained at 200 °C by a thermal auxiliary. The ^{1}D GC oven was ramped from 35 °C to 240 °C at a rate of 5 °C/min and held for an additional 5 min. No ^{2}D oven was used. The modulation period (PM) was 5 s with an 800 ms hot pulse duration. The helium carrier gas (high purity ALPHAGAZ™, Air Liquide, Liège, Belgium) was held at a constant flow rate of 1.0 mL/min. The HRTOF-MS was operated in electron ionization (EI) mode with an ionizing voltage of 70 V. An acquisition rate of 50 Hz was used with a mass range of 30–400 m/z and an acquisition delay of 1 min. The plate voltage was 2150 V with a sampling interval of 0.25 µs. Data were acquired using MassCenter version 2.6.2b (JEOL Ltd.). Instrument tuning was performed using perfluorokerosene (PFK) (Tokyo Chemical Industry Co. Ltd., Tokyo, Japan) and the mass resolution was above 7000 at m/z 293. Data was analysed in GC Image 2.5 HR (Zoex Corporation) using the GC Project and Image Investigator features. Compound identification was made by comparison to the 2014 National Institute of Standards and Technology (NIST) library [15].

The data were first exported in Microsoft Excel (Microsoft Corporation, Redmond WA, USA) for the initial matrix creation. Hierarchical Cluster Analysis (HCA) and heat map visualization were performed in the open source software for statistics, R (The R Foundation for Statistical Computing, version 3.1.3, Vienna, Austria).

Not all bodies could be included into the statistical part of the study. For the HCA, body 2 was not used since only two gas reservoirs were available. The clustering analysis of two samples is irrelevant. For the heat map processing, body 3 was not used because the analytical conditions were slightly different from the other samples.

3. Results and Discussion

3.1. Chromatographic Considerations and Data Processing

The chromatogram displayed in Figure 1 was acquired on a classical column set (i.e., 5% phenylsiloxane—50% phenylsiloxane). Further tests were also conducted using an Rxi-624Sil MS (30 m × 0.25 mm ID × 1.4 µm df)—Stabilwax (2 m × 0.25 mm ID × 0.5 µm df) (Restek Corporation) combination, as already applied in previous decomposition studies [11]. The peak shape and the artifact level improved when using the Rxi-624Sil MS—Stabilwax column set. However, since a second sampling was not possible due to restricted access to samples, the classical column set was used for this proof-of-concept study, and future studies will utilize other column combinations that may be more beneficial to chromatographic qualities. To overpass the chromatographic issues in this data set (e.g., tailing, siloxane background, etc.), a robust alignment process was necessary.

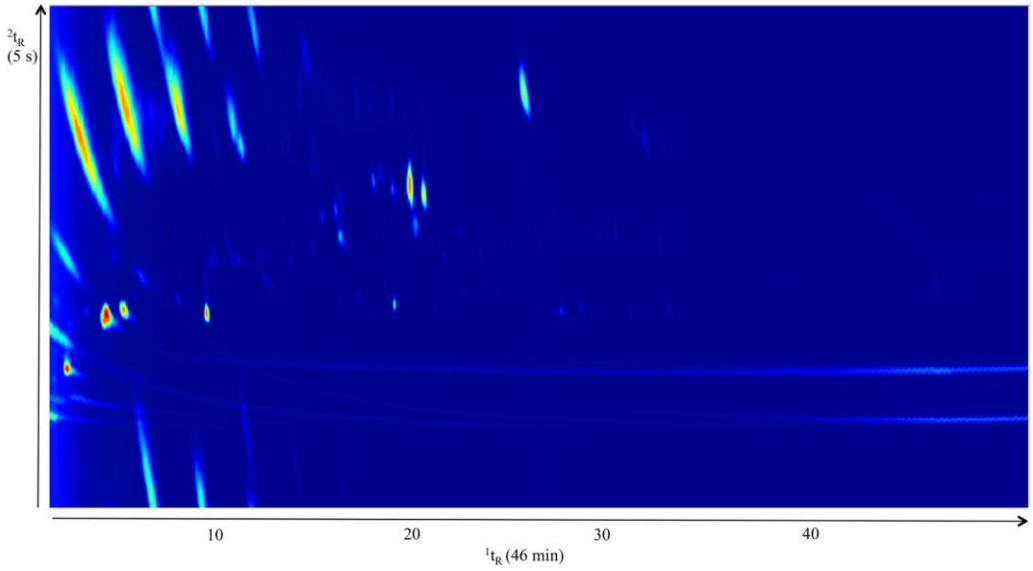

Figure 1. SPME GC×GC-HRTOF-MS total ion current (TIC) chromatogram (30 m × 0.25 mm ID × 0.25 µm df Rxi-5Sil MS as ^{1}D and 2.0 m × 0.25 mm ID × 0.25 µm df Rxi-17Sil MS as ^{2}D) of the pericardium cavity gas sample collected from body 1 (see Table 1).

The first step of data processing was to pre-process each chromatogram for baseline correction, peak detection, and phase shift in order to improve chromatogram alignment. Following these steps, the processed images were used and summed to generate a cumulative image and a feature template from the aligned chromatograms (Figure 2). Every feature designated in the feature template was manually reviewed in order to check the assignment and peak shape for each compound and remove chromatographic artifacts from the template. The resulting template was then applied to all of the samples and the generated data matrix was exported as a *.csv file. This data processing approach was conducted for every comparison. In the absence of these template control steps, there would

have been a number of unfortunate outcomes including: multiple peak identifications for a single chromatographic peak, peak misidentification, and assignment of non-relevant peaks as components of internal gas.

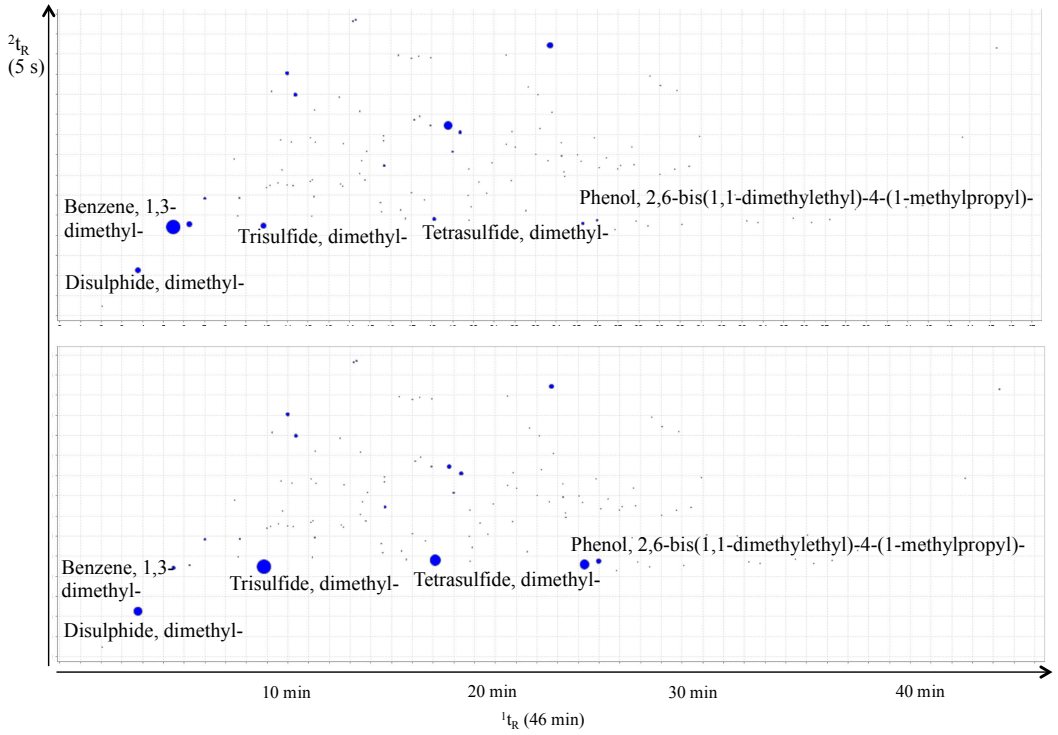

Figure 2. Apex plot of the cumulative image used in the inter-body comparison. On the top, the size of the blobs represents the area of the peak. On the bottom one, the size is proportional to the Fisher Ratio (FR) value. The most intense peaks are not always the most variable.

3.2. Intra-Body Analysis

First, the intra-body variation was investigated considering gas samples collected from various cavities in same individuals. HCA was performed to highlight possible differences between gas reservoir locations in a single body. As illustrated in the corresponding dendrograms (Figure 3), the arrangement after hierarchical clustering underlines the difference between gas samples while showing apparent similarities between VOC profiles issued from samples. For all HCA analyses conducted herein, peak area values were transformed using *z*-score normalization, and Euclidean distances were calculated based on these values. For each body, the data set contained between 60 and 100 compounds. Figure 3 illustrates two examples of the typical output obtained using this method. For the cluster tree of body 1, the two most closely related VOC profiles resulted from samples originating from the lungs. This is consistent with the hypothesis of tissue-specific degradation processes reported in previous studies [17,23]. Following the lung samples, the pectoral muscle, the abdominal cavity, and the pericardium exhibited decreasing similarities, based on the Euclidean distances. Similar results were also obtained for body 3, whereby the thoracic cavity samples were the most comparable to each other, although the abdominal cavity and the heart were less similar to these. For body 4, a different trend was observed using HCA. The pectoral muscle and jugular were the most similar to each other, followed by the subcutaneous gluteal tissue and pericardium samples. The abdominal cavity appeared to be the most different sample in the case of body 4. Based on these preliminary results, the similarity of samples did not follow the same trends across all bodies investigated. Some of the sampling locations (i.e., organ containing a gas reservoir) were comparable in both cases; however, they did not cluster in the same way on the HCA dendrogram. Due to the fact that there are a variety of extraneous

factors that can influence decomposition VOC profiles, it is hypothesized that the differences in trends could be resulting from various postmortem factors (e.g., cause of death, postmortem interval, location of death [24–27]) or antemortem factors (e.g., health conditions, origin, lifestyle, gender, height, weight, diet, medications taken) which can both influence the thanatomicrobiome responsible for alteration gas generation [28]. In the case of body 4, the body was in a fresher state of decomposition compared to body 1 and body 3 (Table 1); therefore, it is suspected that one of the major contributing factors to the difference in trends within each body was likely the PMI.

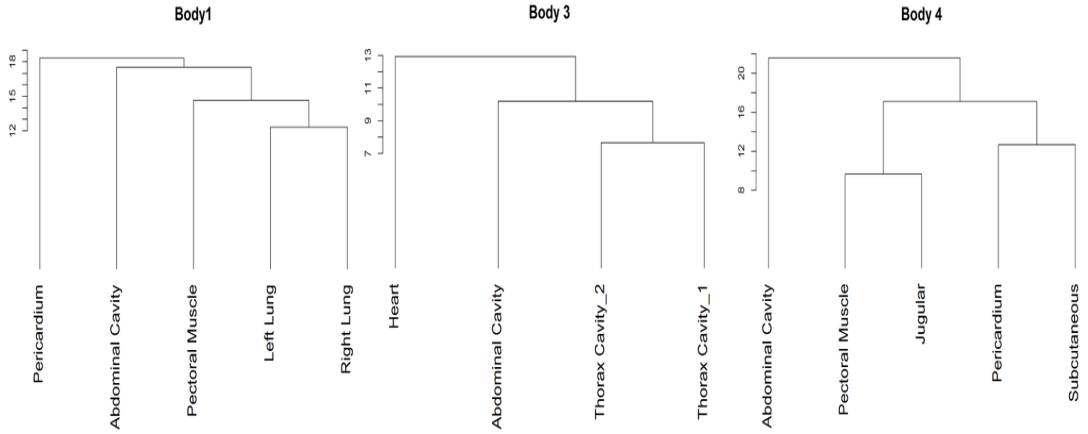

Figure 3. Hierarchical Cluster Analysis (HCA) dendrogram based on the Euclidian distances of *z*-score normalized peak areas for three different cadavers. Segregation based on full volatile organic compound (VOC) profiles measured in each gas reservoirs.

Because the peak table corresponding to the template chromatogram listed several sulfide compounds at significant relative levels, the clustering behavior observed in Figure 3 was investigated based on the level of these sulfide compounds. As illustrated in Figure 4, a relationship appeared to exist between the level of sulfide VOCs and the clusters of bodies observed on the HCA dendrograms (Figure 3). For body 1, the pericardium sample contained high levels of dimethyl trisulfide and dimethyl tetrasulfide (Figure 4). The abdominal cavity, the pectoral muscle, and the lungs exhibited decreasing levels of sulfides respectively (Figure 4). For Body 4, the first two clusters (i.e., pericardium/subcutaneous gluteal muscle and pectoral muscle/jugular vein) (Figure 3) displayed similar levels of sulfide compounds (Figure 4), especially dimethyl disulfide, dimethyl trisulfide and dimethyl tetrasulfide. The abdominal cavity differed in comparison to these first two clusters (Figure 3) based on higher levels of these three compounds. Similar results were obtained for body 3. Perrault et al. [29] have also discussed the importance of the polysulfide compounds in the monitoring of decomposition VOCs. Indeed, the presence of these compounds at different levels throughout the decomposition promoted them as potential PMI indicators [29]. The mass spectral identification of the sulfide compounds was facilitated by the specific isotopic pattern obtained from the sulfur component on the corresponding mass spectrum. Scripting on such mass spectral feature can easily be implemented for rapid identification of sulfides. Moreover, these compounds could be interesting for the development of routine forensic screening methods, since sulfur-specific detectors are also commercially available and come with reduced cost and higher portability compared to mass spectrometers [30].

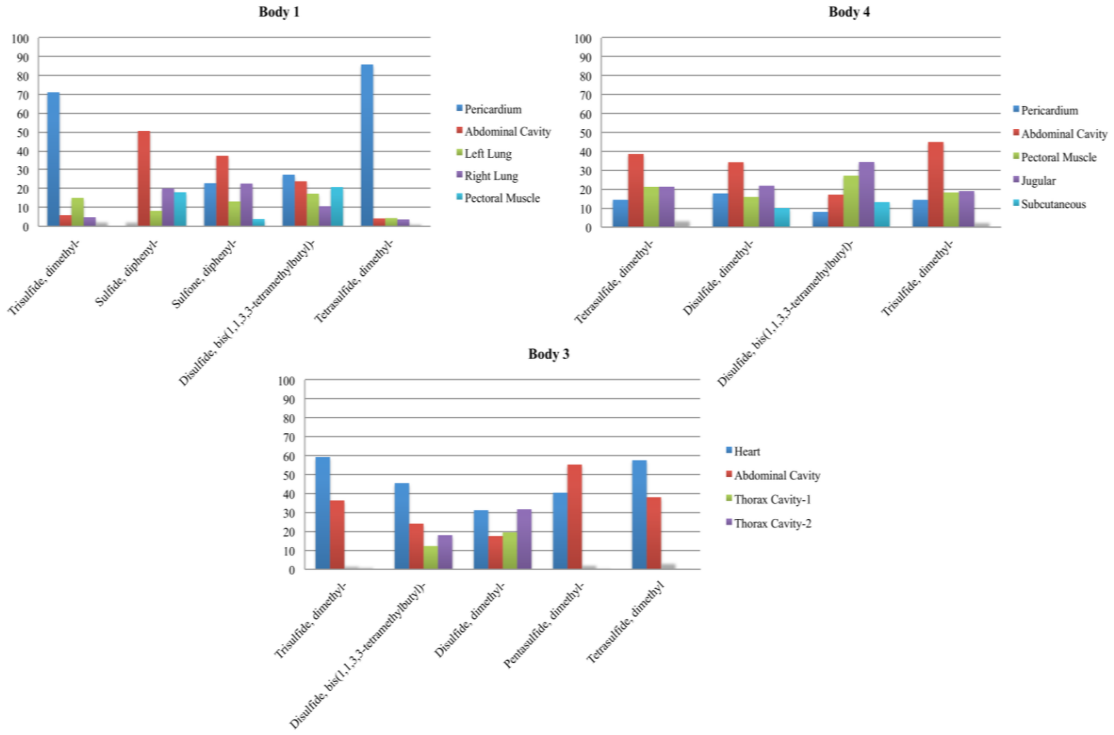

Figure 4. Relative levels of major sulfide compounds based on normalized relative peak area for each compound.

3.3. Inter-Body Analysis

The next stage of this study was to compare the inter- and intra-body differences. Data were reprocessed grouping samples by bodies rather than by sampling localization. Each body was defined as a class of samples. For all compounds remaining after data alignment, Fisher Ratios (FR) were calculated [31]. These FR values were compared to the F critical value (F_{crit}) defined regarding the number of classes, degrees of freedom, and a confidence interval of 99%. Compounds with a FR exceeding F_{crit} were retained and defined as being compounds of interest for the differentiation of bodies. This data analysis approach has been previously reported to be efficient for handling complex multivariate GC×GC data [13,32]. This approach allows data reduction without loss of information, therefore leading to extraction of the most pertinent variables and removal of artifacts that do not discriminate the variables under examination. This data reduction step is necessary due to the fact that GC×GC allows the detection of a large number of compounds, generating high dimensionality matrices that are not ideal for classical statistics. Out of the 102 analytes present in the template list, the process extracted a set of 37 analytes that were the most specific amongst the different classes.

HCA was performed on the resulting matrix of analytes and results can be visualized in the tree-structured graph (left) and heat map (right) of Figure 5. In the heat map, each of the 37 analytes is displayed along the *x*-axis and the amount of each of them is coded based on a color scale. The *y*-axis lists the different bodies. The dendrogram on the left clusters samples originating from the same body together. Based on Figure 5, it appeared that the inter-body variation exceeded the organ-to-organ variation. Two samples originating from two different areas within the same body were therefore more similar to each other than two samples collected from the same location in two different bodies. The abundance of compounds was lowest in body 4, with the exception of A27 which had the highest concentration in this body compared with other samples collected from different bodies. The variation observed in body 1 and body 2 could potentially be related to the different postmortem intervals of the bodies, since they were in different states of decomposition. This observation could indicate that internal VOC monitoring may have potential in estimating PMI in the future. Regardless of

the position of the internal gas reservoir, the chemical composition appeared to be related to the state of decomposition. Due to the limited number of cadavers in this study and limited knowledge regarding the exact postmortem interval of each body, further statistical correlation between PMI and chemical composition was not possible. However, future studies will endeavor to provide more details regarding this point and will also attempt to elucidate specific VOC compounds that may fluctuate in a reproducible pattern to allow PMI estimation using this procedure.

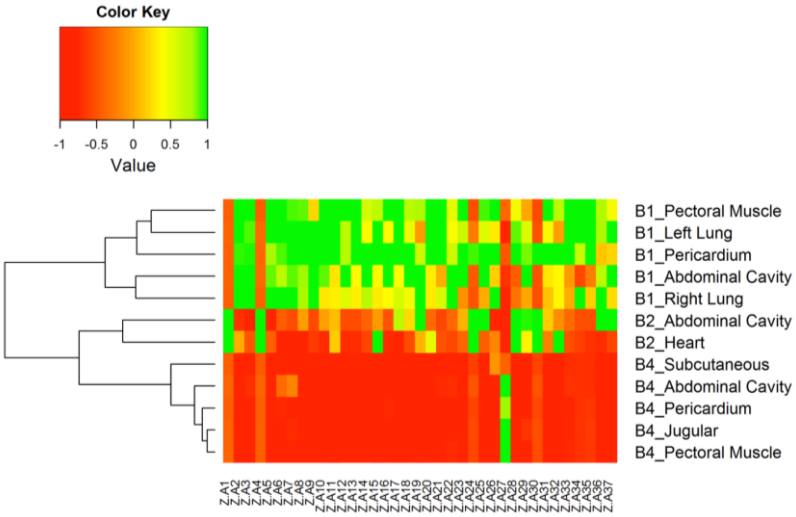

Figure 5. Hierarchical cluster analysis (HCA) heat map representation using the Euclidian distance between the *z*-score for each compound of interest detected from the gas reservoirs within three cadavers. The compound labels along the *x*-axis are listed in Table 1a,b (e.g., Z-A18 indicates the *z*-score based on compound A18, p-Cymene). B1: Body 1, B2: Body 2, B3: Body 3.

The 37 compounds of the heat map in Figure 5 are listed in Table 2a,b. All of these compounds of interest were first identified using mass spectral library searches. From these 37 compounds, 17 identifications were further supported by high-resolution mass spectral information with mass accuracy values lower than 30 ppm (Table 2a). To calculate the mass accuracy, the drift mass was corrected based on the siloxane peak (m/z 207.0329), taken directly beside the corresponding compound peak. The identified decomposition-specific VOCs were polysulfide compounds (dimethyl trisulfide and dimethyl tetrasulfide) [33], different isomers of xylene and cymene, as well as phenolic compounds [8,33,34].

The HRTOF-MS used in this study was operated using an electron ionization source, which does not provide the molecular ion for less stable compounds (e.g., long hydrocarbon chains, oxygenated compounds). For some of the compounds, either the parent ion or ions resulting from the loss of small masses (e.g., CH_3, H_2O) can be of sufficient specificity for mass error calculation, and these can be used to support library identifications. However, for less stable compounds, soft ionization techniques would be much more beneficial in the future to be able to calculate the chemical formula using the molecular ion. Table 2b lists the compounds that were identified by mass spectral library searching but for which identities were not further supported by high-resolution mass spectral formula calculation. For some of them, no compound names are therefore listed in Table 2b because the library identification was clearly incorrect as the compound position on the GC×GC space was wrong. For example, A27 was 'identified' as a branched cyclohexane; however, the second dimension retention time (^2t_R = 3.3 s) was too long for this type of compound. A formula simulation, run using the highest mass of the spectra, did not provide a more reliable identification, and therefore these compounds were represented separately from those in Table 2a. Nevertheless, some compounds (e.g., A10 and A37) had sufficient matches with libraries that they could be considered as acceptable for a proof-of-concept study, although such identities will require further validation in the future.

Table 2. (**a**) Compounds with identification supported by high-resolution mass spectral information. (**b**) Compound identifications not supported by high-resolution mass spectral information.

(a)

Label	Compound Name	$^{1}t_R$ (min)	$^{2}t_R$ (s)	FR	Match	Reverse	Probability	Formula	Exact Mass (amu)	Corrected Mass (amu)	Measured Mass (amu)	Accuracy (ppm)
A1	Cyclic octaatomic sulfur	35.6	1.7	294.1	548	552	90.66	S_8	223.8045	223.7791	223.7777	6.06
A2	Azulene	16.5	2.1	143.8	932	932	53.88	$C_{10}H_8$	128.0626	128.0432	128.0458	−20.68
A3	Benzene, 1-methyl-3-(1-methylethyl)-	11.0	2.4	127.1	899	899	14.34	$C_{10}H_{14}$	134.1096	134.0901	134.0913	−8.93
A4	Hexathiepane	34.0	1.7	119.7	758	796	98.87	CH_2S_6	205.8481	205.8226	205.8233	−3.24
A5	Benzene, 1-ethyl-2,4-dimethyl-	11.3	2.4	80.7	882	890	17.39	$C_{10}H_{14}$	134.1096	134.0901	134.0919	−13.41
A6	Benzene, 1,3-dimethyl-	5.5	1.9	55.0	832	862	23.85	C_8H_{10}	106.0783	106.0650	106.0639	10.39
A7	Benzene, 1,4-dimethyl-	6.3	1.9	54.2	877	881	25.07	C_8H_{10}	106.0783	106.0750	106.0718	30.19
A9	Benzene, 1,2,3,5-tetramethyl-	12.2	2.5	45.4	856	880	15.1	$C_{10}H_{14}$	134.1096	134.0901	134.0927	−19.38
A13	1H-Indene, 2-butyl-5-hexyloctahydro-	23.8	4.1	24.2	672	676	7.27	$C_{19}H_{36}$	249.2582	249.2328	249.2282	18.36
A14	Phenol, 2,6-bis(1,1-dimethylethyl)-4-(1-methylpropyl)-	25.0	2.8	24.0	787	794	7.53	$C_{18}H_{30}O$	262.2297	262.2042	262.2002	15.32
A18	p-Cymene	13.5	2.5	21.0	581	634	10.41	$C_{10}H_{14}$	134.1096	134.0901	134.0915	−10.43
A19	p-Isopropenylphenol	19.8	2.0	20.8	892	905	60.64	$C_9H_{10}O$	134.0732	134.0537	134.0551	−10.32
A22	Phenol, 4,4′-(1-methylethylidene)bis-	41.7	2.2	16.9	884	964	82.47	$C_{15}H_{16}O_2$	228.1150	228.0956	228.0940	6.94
A24	Trisulfide, dimethyl-	9.8	1.9	16.8	725	741	88.51	$C_2H_6S_3$	125.9632	125.9377	125.9341	28.73
A28	Benzene, 1,3-bis(1,1-dimethylethyl)-	14.9	2.9	12.2	914	917	76.52	$C_{14}H_{22}$	190.1722	190.1527	190.1496	16.31
A30	Tetrasulfide, dimethyl-	18.1	2.0	10.5	742	742	55.43	$C_2H_6S_4$	157.9352	157.9320	157.9306	8.80
A32	Phenol, 2-(1,1-dimethylethyl)-5-methyl-	19.8	2.3	9.6	885	885	26.9	$C_{11}H_{16}O$	164.1201	164.1007	164.1000	4.06

(b)

Label	Compound Name	$^{1}t_R$ (min)	$^{2}t_R$ (s)	FR	Match	Reverse	Probability	Formula
A8	Sulfurous acid, cyclohexylmethyl isobutyl ester	28.4	3.8	46.6	630	803	16.3	$C_{11}H_{22}O_3S$
A10	2-Bromobenzothiazole	27.8	2.7	36.1	812	892	70.5	C_7H_4BrNS
A11	1,2,3-Trimethyl-cyclopent-2-enecarboxaldehyde	17.1	3.2	27.2	619	724	10.3	$C_9H_{14}O$
A12	Stiripentol	29.8	2.6	26.1	661	673	39.91	$C_{14}H_{18}O_3$
A15	1,2-Diazaspiro[4.4]nonen-3-carboxylic acid, 6,6,9,9-tetramethyl-, methyl ester	17.4	3.3	22.1	605	690	9.55	$C_{13}H_{22}$
A16	Phthalic acid, methyl phenyl ester	27.0	2.6	22.0	748	836	5.57	$C_{10}H_{10}$
A17	2-Dodecen-1-yl(-)succinic anhydride	18.8	3.2	21.3	576	671	17.82	$C_{16}H_{26}O_3$
A20	Neophytadiene	16.9	4.1	20.7	676	715	7.4	$C_{20}H_{38}$
A21	3-Tetradecyn-1-ol	20.9	2.7	20.5	687	692	24.49	$C_{14}H_{26}O$
A23	Vinyl caprylate	23.9	3.3	16.9	601	623	8.39	$C_{10}H_{18}O_2$
A25	Disulfide, bis(1,1,3,3-tetramethylbutyl)	16.4	4.0	15.5	760	766	46.1	$C_{16}H_{34}S_2$
A26	Benzoic acid, 3,5-dimethyl-, (2,4-dimethylphenyl)methyl ester	15.5	2.2	13.7	761	761	27.59	$C_{18}H_{20}O_2$
A27	Cyclohexane, 2,4-diisopropyl-1,1-dimethyl-	18.5	3.3	12.4	530	678	8.35	$C_{12}H_{24}$
A29	Vinyl caprylate	15.7	3.0	11.2	714	725	25.61	$C_{10}H_{18}O_2$
A31	Neophytadiene	11.4	3.5	10.2	717	774	4.96	$C_{20}H_{38}$
A33	4-imidazolidinone, 3-ethyl-5-[2-(3-ethyl-2(3H)-benzoxazolylidene)ethylidene]-1-phenyl-2-thioxo-	14.2	4.4	9.6	492	770	41.69	$C_{22}H_{21}N_3O_2S$
A34	4-Hepten-3-one, 5-methyl-. (E)-	19.3	3.1	9.3	599	665	5.96	$C_8H_{14}O$
A35	Sulfurous acid, cyclohexylmethyl isobutyl ester	29.8	3.6	9.3	630	801	16.6	$C_{11}H_{22}O_3S$
A36	Succinic acid, 2-(2-chlorophenoxy)ethyl ethyl ester	31.0	1.9	8.9	612	626	34.43	$C_{14}H_{17}ClO_5$
A37	2,4,6-Tris(1,1-dimethylethyl)-4-methylcyclohexa-2,5-dien-1-one	22.8	2.6	8.7	803	857	31.2	$C_{19}H_{32}O$

4. Conclusions

This proof-of-concept study demonstrates the potential of monitoring volatile organic compounds from human intracadaveric gas reservoirs. The precision of PMCT scanning for gas reservoirs within a body combined with the analytical power of SPME GC×GC-HRTOF-MS allowed a non-destructive, non-targeted screening of these volatile samples. The chemical composition of these gas reservoirs may have the potential to provide important information about the decomposition state of a body, and could therefore lead to potential enhancement of PMI estimation based on the use of additional taphonomic markers that would be valuable during early stage decomposition. A trend to different volatile patterns was also observed for each organ, indicating a possible specific decomposition pathway for each of them. The sulfide compounds appeared to be an important class of compounds for ascertaining these differences. An inter-body comparison demonstrated that the variation between individuals exceeds the variation between samples collected from a single individual. This observation is a major point of interest since it could help to develop new techniques for PMI estimation during early decomposition, where few non-invasive techniques are available. Future work will aim to increase the number of individuals studied in order to identify key VOCs that are related to the state of decomposition. A larger data set will also assist with further supporting tentative identifications of some compounds made herein. The purpose of performing this non-targeted analysis will aid in identifying several compounds that can further be investigated in targeted studies. In this case, a quantification method would also be valuable, especially for the sulfide compounds that appear to have potential as decomposition stage markers.

Acknowledgments: We would like to thank JEOL (Europe) B.V. (Niew-Vennep, The Nederlands) for strong instrumental and technical support. We also thank Restek® Corporation (Bellefonte, PA, USA) and Sigma Aldrich® (St. Louis, MO, USA) for providing us with GC phases, SPME fibers, and various GC consumables.

Author Contributions: J.-F.F., P.-H.S., S.G. and V.V. conceived and designed the experiments; P.-H.S., K.A.P. and V.V. performed the experiments; P.-H.S. analyzed the data and wrote the paper; J.-F.F., K.A.P., S.G. and V.V. performed manuscript corrections and edits.

Conflicts of Interest: The authors declare no conflict of interest.

Abbreviations

The following abbreviations are used in this manuscript:

MDCP	multi-detector computed tomography
VOCs	volatile organic compounds
GC×GC	comprehensive two-dimensional gas chromatography
HRTOF-MS	time of flight high-resolution mass spectrometry
PMI	postmortem interval
SPME	solid phase microextraction
PDMS	polydimethylsiloxane
^{1}D	first dimension
^{2}D	second dimension
1D GC	one-dimensional gas chromatography
PM	modulation period
EI	electron ionization
PFK	perfluorokerozene
HCA	hierarchical cluster analysis
TIC	total ion current
FR	Fisher ratio
F_{crit}	F critical
$^{1}t_R$	1st dimension retention time
$^{2}t_R$	2nd dimension retention time

References

1. Jacobsen, C.; Lynnerup, N. Craniocerebral trauma—Congruence between post-mortem computed tomography diagnoses and autopsy results. *Forensic Sci. Int.* **2010**, *194*, 9–14. [CrossRef] [PubMed]
2. Roberts, I.S.D.; Benamore, R.E.; Benbow, E.W.; Lee, S.H.; Harris, J.N.; Jackson, A.; Mallett, S.; Patankar, T.; Peebles, C.; Roobottom, C.; et al. Post-mortem imaging as an alternative to autopsy in the diagnosis of adult deaths: A validation study. *Lancet* **2012**, *379*, 136–142. [CrossRef]
3. Kasahara, S.; Makino, Y.; Hayakawa, M.; Yajima, D.; Ito, H.; Iwase, H. Diagnosable and non-diagnosable causes of death by postmortem computed tomography: A review of 339 forensic cases. *Legal Med.* **2012**, *14*, 239–245. [CrossRef] [PubMed]
4. Varlet, V.; De Croutte, E.L.; Augsburger, M.; Mangin, P. A new approach for the carbon monoxide (CO) exposure diagnosis: measurement of total CO in human blood versus carboxyhemoglobin (HbCO). *J. Forensic Sci.* **2013**, *58*, 1041–1046. [CrossRef] [PubMed]
5. Varlet, V.; Giuliani, N.; Palmiere, C.; Maujean, G.; Augsburger, M. Hydrogen sulfide measurement by headspace-gas chromatography-mass spectrometry (HS-GC-MS): Application to gaseous samples and gas dissolved in muscle. *J. Anal. Toxicol.* **2015**, *39*, 52–57. [CrossRef] [PubMed]
6. Banaschak, S.; Janßen, K.; Becker, K.; Friedrich, K.; Rothschild, M.A. Fatal postpartum air embolism due to uterine inversion and atonic hemorrhage. *Int. J. Legal Med.* **2013**, *128*, 147–150. [CrossRef] [PubMed]
7. Brasseur, C.; Dekeirsschieter, J.; Schotsmans, E.M.J.; de Koning, S.; Wilson, A.S.; Haubruge, E.; Focant, J.-F. Comprehensive two-dimensional gas chromatography-time-of-flight mass spectrometry for the forensic study of cadaveric volatile organic compounds released in soil by buried decaying pig carcasses. *J. Chromatogr.* **2012**, *1255*, 163–170. [CrossRef] [PubMed]
8. Perrault, K.; Stuart, B.; Forbes, S. A longitudinal study of decomposition odour in soil using sorbent tubes and solid phase microextraction. *Chromatography* **2014**, *1*, 120–140. [CrossRef]
9. Forbes, S.L.; Perrault, K.A. Decomposition odour profiling in the air and soil surrounding vertebrate carrion. *PLoS ONE* **2014**, *9*. [CrossRef] [PubMed]
10. Perrault, K.A.; Stefanuto, P.-H.; Stuart, B.H.; Rai, T.; Focant, J.-F.; Forbes, S.L. Reducing variation in decomposition odour profiling using comprehensive two-dimensional gas chromatography. *J. Sep. Sci.* **2014**, *38*, 73–80. [CrossRef] [PubMed]
11. Stefanuto, P.-H.; Perrault, K.A.; Lloyd, R.M.; Stuart, B.; Rai, T.; Forbes, S.L.; Focant, J.-F. Exploring new dimensions in cadaveric decomposition odour analysis. *Anal. Methods* **2015**, *7*, 2287–2294. [CrossRef]
12. Dekeirsschieter, J.; Stefanuto, P.-H.; Brasseur, C.; Haubruge, E.; Focant, J.-F. Enhanced characterization of the smell of death by comprehensive two-dimensional gas chromatography-time-of-flight mass spectrometry (GC×GC–TOFMS). *PLoS ONE* **2012**, *7*. [CrossRef] [PubMed]
13. Stefanuto, P.-H.; Perrault, K.A.; Stadler, S.; Pesesse, R.; LeBlanc, H.N.; Forbes, S.L.; Focant, J.-F. GC×GC–TOFMS and supervised multivariate approaches to study human cadaveric decomposition olfactive signatures. *Anal. Bioanal. Chem.* **2015**, *407*, 4767–4778. [CrossRef] [PubMed]
14. Stefanuto, P.-H.; Perrault, K.; Stadler, S.; Pesesse, R.; Brokl, M.; Forbes, S.; Focant, J.-F. Reading cadaveric decomposition chemistry with a new pair of glasses. *Chem. Plus Chem.* **2014**, *79*, 786–789. [CrossRef]
15. Stadler, S.; Stefanuto, P.-H.; Brokl, M.; Forbes, S.L.; Focant, J.-F. Characterization of volatile organic compounds from human analogue decomposition using thermal desorption coupled to comprehensive two-dimensional gas chromatography-time-of-flight mass spectrometry. *Anal. Chem.* **2013**, *85*, 998–1005. [CrossRef] [PubMed]
16. Focant, J.-F.; Stefanuto, P.-H.; Brasseur, C.; Dekeirsschieter, J.; Haubruge, E.; Schotsmans, E.; Wilson, A.; Stadler, S.; Forbes, S. Forensic cadaveric decomposition profiling by GC×GC–TOFMS analysis of VOCs. *KazNU Bull. Chem. Ser.* **2013**, *72*, 177–186. [CrossRef]
17. Rosier, E.; Loix, S.; Develter, W.; Van de Voorde, W.; Tytgat, J.; Cuypers, E. The search for a volatile human specific marker in the decomposition process. *PLoS ONE* **2015**, *10*. [CrossRef] [PubMed]
18. Vass, A.A.; Barshick, S.-A.; Sega, G.; Caton, J.; Skeen, J.T.; Love, J.C.; Synstelien, J.A. Decomposition chemistry of human remains: A new methodology for determining the postmortem interval. *J. Forensic Sci.* **2002**, *47*, 542–553. [PubMed]
19. Statheropoulos, M.; Spiliopoulou, C.; Agapiou, A. A study of volatile organic compounds evolved from the decaying human body. *Forensic Sci. Int.* **2005**, *153*, 147–155. [CrossRef] [PubMed]

20. Varlet, V.; Smith, F.; Giuliani, N.; Egger, C.; Rinaldi, A.; Dominguez, A.; Chevallier, C.; Bruguier, C.; Augsburger, M.; Mangin, P.; et al. When gas analysis assists with postmortem imaging to diagnose causes of death. *Forensic Sci. Int.* **2015**, *251*, 1–10. [CrossRef] [PubMed]
21. Varlet, V.; Smith, F.; de Froidmont, S.; Dominguez, A.; Rinaldi, A.; Augsburger, M.; Mangin, P.; Grabherr, S. Innovative method for carbon dioxide determination in human postmortem cardiac gas samples using headspace-gas chromatography–mass spectrometry and stable labeled isotope as internal standard. *Anal. Chim. Acta* **2013**, *784*, 42–46. [CrossRef] [PubMed]
22. Varlet, V.; Bruguier, C.; Grabherr, S.; Augsburger, M.; Mangin, P.; Uldin, T. Gas analysis of exhumed cadavers buried for 30 years: A case report about long time alteration. *Int. J. Legal Med.* **2014**, *128*, 719–724. [CrossRef] [PubMed]
23. Hoffman, E.; Curran, A.; Dulgerian, N. Characterization of the volatile organic compounds present in the headspace of decomposing human remains. *Forensic Sci. Int.* **2009**, *186*, 6–13. [CrossRef] [PubMed]
24. Dekeirsschieter, J.; Verheggen, F.J.; Gohy, M.; Hubrecht, F.; Bourguignon, L.; Lognay, G.; Haubruge, E. Cadaveric volatile organic compounds released by decaying pig carcasses (*Sus domesticus* L.) in different biotopes. *Forensic Sci. Int.* **2009**, *189*, 46–53. [CrossRef] [PubMed]
25. Kasper, J.; Mumm, R.; Ruther, J. The composition of carcass volatile profiles in relation to storage time and climate conditions. *Forensic Sci. Int.* **2012**, *223*, 64–71. [CrossRef] [PubMed]
26. Vass, A.A. Odor mortis. *Forensic Sci. Int.* **2012**, *222*, 234–241. [CrossRef] [PubMed]
27. Perrault, K.A.; Rai, T.; Stuart, B.H.; Forbes, S.L. Seasonal comparison of carrion volatiles in decomposition soil using comprehensive two-dimensional gas chromatography—Time of flight mass spectrometry. *Anal. Methods* **2014**, *7*, 690–698. [CrossRef]
28. Can, I.; Javan, G.T.; Pozhitkov, A.E.; Noble, P.A. Distinctive thanatomicrobiome signatures found in the blood and internal organs of humans. *J. Microbiol. Methods* **2010**, *106*, 1–7. [CrossRef] [PubMed]
29. Perrault, K.A.; Nizio, K.D.; Forbes, S.L. A comparison of one-dimensional and comprehensive two-dimensional gas chromatography for decomposition odour profiling using inter-year replicate field trials. *Chromatographia* **2015**, *78*, 1057–1070. [CrossRef]
30. Furne, J.; Majerus, G.; Lenton, P.; Springfield, J.; Levitt, D.G.; Levitt, M.D. Comparison of volatile sulfur compound concentrations measured with a sulfide detector vs. gas chromatography. *J. Dent. Res.* **2002**, *81*, 140–143. [CrossRef] [PubMed]
31. Pierce, K.M.; Hoggard, J.C.; Hope, J.L.; Rainey, P.M.; Hoofnagle, A.N.; Jack, R.M.; Wright, B.W.; Synovec, R.E. Fisher ratio method applied to third-order separation data to identify significant chemical components of metabolite extracts. *Anal. Chem.* **2006**, *78*, 5068–5075. [CrossRef] [PubMed]
32. Brokl, M.; Bishop, L.; Wright, C.G.; Liu, C.; McAdam, K.; Focant, J.-F. Multivariate analysis of mainstream tobacco smoke particulate phase by headspace solid-phase micro extraction coupled with comprehensive two-dimensional gas chromatography-time-of-flight mass spectrometry. *J. Chromatogr.* **2014**, *1370*, 216–229. [CrossRef] [PubMed]
33. Armstrong, P.; Nizio, K.D.; Perrault, K.A.; Forbes, S.L. Establishing the volatile profile of pig carcasses as analogues for human decomposition during the early postmortem period. *Heliyon* **2016**, *2*. [CrossRef] [PubMed]
34. Swann, L.M.; Forbes, S.L.; Lewis, S.W. Analytical separations of mammalian decomposition products for forensic science: A review. *Anal. Chim. Acta* **2010**, *682*, 9–22. [CrossRef] [PubMed]